Journal of Applied Sciences

ISSN 1812-5654

science alert

ANSInet
an open access publisher
http://ansinet.com

Journal of Applied Sciences 8 (21): 3845-3853, 2008
ISSN 1812-5654

Evaluate the Validity of Using the Non-Metric Photographs For Documenting Historical Buildings

[1,2]Tarek, M.A., [1]ZHU Qing, [2]Abbas M. El-Din, [2]Essam M. Fawaz, [2]A. Esmat and [2]Said El-Maghraby
[1]State Key Laboratory of Information Engineering in Surveying Mapping and Remote Sensing, Wuhan University, Wuhan 430079, People's Republic of China
[2]Faculty of Engineering, Al-Azhar University, Cairo, Egypt

Abstract: In this study, we will evaluate both of the effect of the number of control points and the effect of the ratio of the base line distance (B) over the object distance (D) [(B/D) ratio] on the accuracy obtained from the ground coordinates using non-metric photographs for documenting historical buildings. A wall of Moid Shikh historical mosque located in Ghoria, beside Bab Ziwala, Cairo, Egypt, is employed as a test object. The data acquisition and the analysis of the results for number of control points and the ratio of the base distance (B) to the object distance (D) [(B/D) ratio] are presented in this study. The results for evaluated the effect of the number of control points on the accuracy obtained from non-metric photographs for documenting historical buildings show, when the number of control points increasing, the accuracy is increasing. Also, the effect of [(B/D) ratio] on the accuracy shows the relations Y, Z and R direction are directly proportionally in the range of $0.5 \leq (B/D)\ \text{ratio} \leq 1.0$, while the relations are inversely proportionally in the range of $1.0 \leq (B/D)\ \text{ratio} \leq 1.5$. Only the relation in X-direction is not matched with the other relations.

Key words: Close-range photogrammetry, non-metric photos, documenting buildings, control points, (B/D) ratio

INTRODUCTION

In many cases the choice of the technique used in recording building depends on the historical value, the available instrument and the field circumstance for this building. Many techniques used for documenting buildings, photogrammetry is one of these techniques. Photogrammetry has been defined by the American Society for Photogrammetry and Remote Sensing as the art, science and technology of obtaining reliable information about physical objects and the environment through processes of recording, measuring and interpreting photographic images and patterns of recorded radiant electromagnetic energy and other phenomena (Mofitt and Mikhail, 1980; Wolf and DeWitt, 2000; Atkinson, 2001). In photogrammetry the object is recorded on an intermediate medium, such as photographs and the measurements are carried out later in the office. Photogrammetry is generally accepted technique for collection of the three-dimensional representations of the environment. This technique has also been extensively used for documentation different building (Karara and Abdel-Aziz, 1974; Nutto and Ringle, 2001).

Close-range photogrammetry can be achieving the photos by Metric camera or Non-Metric camera. In last years, Non-Metric cameras were very common for documenting buildings. Non-metric cameras are defined as cameras that are not specifically designed for photogrammetric purposes or a camera whose interior orientation is completely or partially, unknown and unstable. Off-the-shelf, amateur and professional cameras fall into this category. Jechev describes some problems for using non-metric cameras for photogrammetric purposes and the solving of these problems by using three different methods (Jechev, 2004).

To recreate the shape of buildings, we need at least one Stereomodel-two photographs for each building. In this paper we will evaluate both of the effect of the number of control points as well as the effect of the ratio of the base line distance (B) over the object distance (D) [(B/D) ratio] on the accuracy the data acquisition obtained from Non-Metric photographs.

EXPERIMENTAL WORK

In this case, we choice a wall which about 20 m height and 48 m width (Fig. 1) of Moid Shikh historical mosque

Corresponding Author: Tarek, M.A., State Key Laboratory of Information Engineering in Surveying Mapping and Remote Sensing, Wuhan University, Wuhan 430079, People's Republic of China

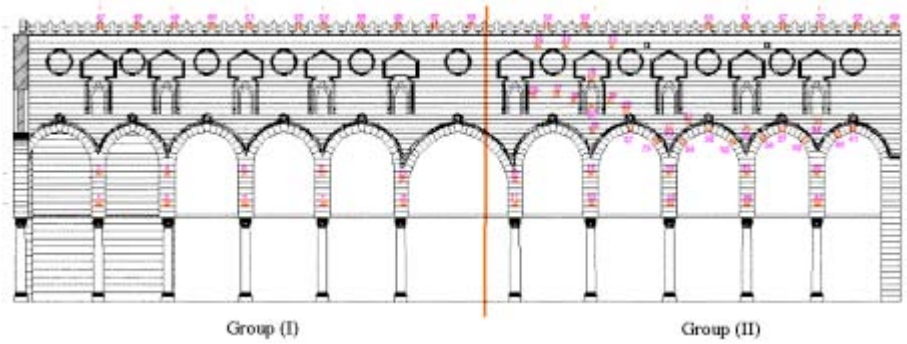

Fig. 1: The two groups (I) and (II) of targets points on historical wall

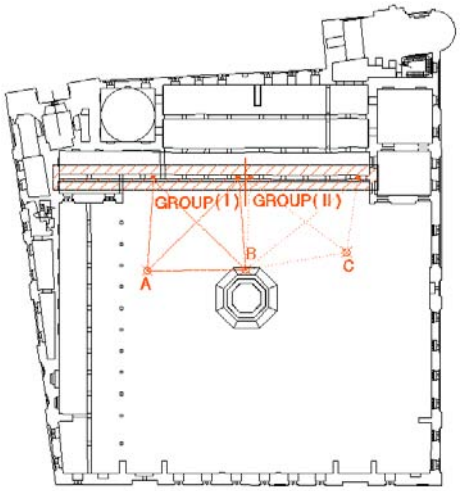

Fig. 2: Sketch of Moid Shikh historical mosque and the locations of the observation stations

located in Ghoria, beside Bab Ziwala, Cairo, Egypt (Fig. 2) to apply our study. Sixty-four targets (20×20 cm) were fixed on the wall of Moid Shikh historical mosque (Fig. 1, 3).

The intersection method was used to calculate the ground coordinates (X_G, Y_G, Z_G) which have been assumed to be a corrected coordinates (i.e., coordinates without error), according to the next assumption:

- The Theodolite used in the observations was a calibrated one-second Theodolite (wild T2) with accuracy (±0.8")
- The angles have been measured at four positions of directions (i.e., the angles were measured eight times)
- The good experience of the observer

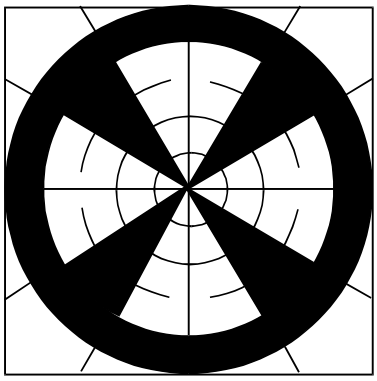

Fig. 3: Sketch for fixed target at the historical wall of Moid Shikh mosque

- The weather through the fieldwork was clear and suitable to get accurate measurements and consequently to obtain high accuracy
- The data reduction used to get the ground coordinates was designed to obtain high accuracy
- The all data was adjusted with least square adjustment

The observations of Theodolite (i.e., The intersection Method) had been done by occupying the available three station points (A, B, C) as shown in Fig. 2, while in the non-metric camera we choose the exposure stations as close as possible to the stations A, B and C.

The coordinates of the station points (A, B, C) were obtained using a calibrated ordinary total station SOKKIA-powerset 3000 (No. 22518-D21810), which have technical specifications as follows; Standard measuring up to 3 km, Accuracy in measuring distance (± (2+2 ppm *D) mm), accuracy in measuring the horizontal and vertical angles (±3"), minimum reading in measuring distance (1 mm) and minimum reading in measuring angles (1"/5").

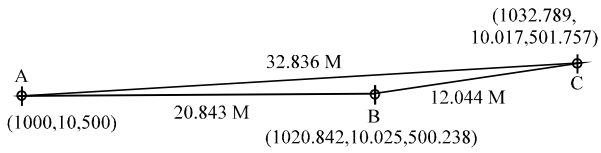

Fig. 4: Plan for location of the station points (A, B, C)

In this study the three axes X, Y and Z were chosen to be as follows: The X and Z axes represent the horizontal plane and the X and Y axes represent the vertical plane.

By Assuming the coordinates of station A = (1000 E, 10 N, 500 Z) and measuring the length and the bearing angle of lines AB and BC tenth times to get the most probable value for stations B and C (Fig. 4).

Theodolite measurements: The measurements have been taken using a calibrated wild T2 one-second theodolite with accuracy = ±0.8". The intersection technique was used to calculate the ground coordinates (X_G, Y_G, Z_G) of each target which have been assumed as a corrected coordinates.

The object (the historical wall of Moid Shikh mosque) has been divided into two groups, group (I), which includes twenty-one targets and group (II), which includes forty-three targets (Fig. 2). Three stations (A, B, C) have been established in the field to apply the intersection technique for the two groups (Fig. 4).

The base line AB was used to obtain the ground coordinates of the targets of group (I) and the base line BC was used to obtain the ground coordinates of the targets of group (II). To obtain the ground coordinates for any target we measure the base distance (B), the horizontal angles (ϕ_A, ϕ_B) and the vertical angels (θ) at each end of the base line (Fig. 5).

The most probable values and their mean square errors (m.s.e) for the horizontal angles have been measured at four positions of directions (0, 45, 90 and 135°), for each position the angle had been measured face left and face right (i.e., each angle had been measured eight times). The most probable values of the horizontal angles and their m.s.e were founded for group I and II. In group I one target was not observed, while in group II eight targets were not observed because of some obstacles in pointing these targets. The mathematical model of coordinate computations is based on the following three equations:

$$X_G = X_A + \frac{L_{AB} \times \sin\phi_B}{\sin(\phi_A + \phi_B)}[\sin(\phi_{AB} - \phi_A)] \quad (1)$$

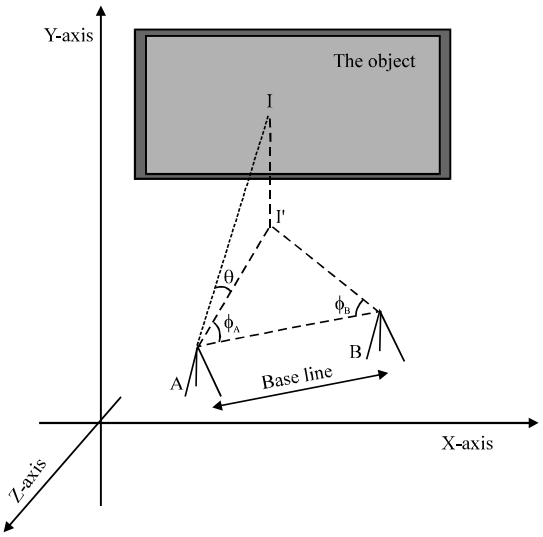

Fig. 5: Explain the intersection method, which used to obtain the space coordinates of the targets

$$Y_G = Y_A + h_i + \frac{L_{AB} \times \sin\phi_B}{\sin(\phi_A + \phi_B)}[\tan\theta] \quad (2)$$

$$Z_G = Z_A + \frac{L_{AB} \times \sin\phi_B}{\sin(\phi_A + \phi_B)}[\cos(\phi_{AB} - \phi_A)] \quad (3)$$

Where:

A, B	:	The two end points of the base line
X_A, Y_A, Z_A	:	The ground coordinates of point (A)
X_B, Y_B, Z_B	:	The ground coordinates of point (B)
L_{AB}	:	The base line length (measuring accuracy ± 2.0 mm)
ϕ_A	:	The horizontal angle measured from point (A) (measuring accuracy ± 5")
ϕ_B	:	The horizontal angle measured from point (B) (measuring accuracy ± 5")
ϕ_{AB}	:	The bearing angle for base line (AB) (measuring accuracy ± 5")
θ	:	The vertical angle measured from point (A) (measuring accuracy ± 5")
h_i	:	The height of Theodolite

To simplify the calculations, an Excel program was achieved INTERSECTION program features can be summarized as follows:

- The result of the mathematical model of computing the coordinates is given in Eq. 1-3
- It can accept the measured horizontal and vertical angles to each target, as measured from the two ends of the base line

Accuracy of the coordinates is estimated using the theorem of error propagation. According to error propagation theorem Eq. 1-3 must be partially differentiated with respect to each measured variable (L_{AB}, ϕ_A, ϕ_B and θ).

$$[\sigma(X_G)]^2 = (\frac{\delta X_G}{\delta L_{AB}})^2 \times [\sigma(L_{AB})]^2 + (\frac{\delta X_G}{\delta \phi_A})^2 \times [\sigma(\phi_A)]^2 + (\frac{\delta X_G}{\delta \phi_B})^2 \times [\sigma(\phi_B)]^2 \quad (4)$$

$$[\sigma(Y_G)]^2 = (\frac{\delta Y_G}{\delta L_{AB}})^2 \times [\sigma(L_{AB})]^2 + (\frac{\delta Y_G}{\delta \phi_A})^2 \times [\sigma(\phi_A)]^2 + (\frac{\delta Y_G}{\delta \phi_B})^2 \times [\sigma(\phi_B)]^2 + (\frac{\delta Y_G}{\delta \theta})^2 \times [\sigma(\theta)]^2 \quad (5)$$

$$[\sigma(Z_G)]^2 = (\frac{\delta Z_G}{\delta L_{AB}})^2 \times [\sigma(L_{AB})]^2 + (\frac{\delta Z_G}{\delta \phi_A})^2 \times [\sigma(\phi_A)]^2 + (\frac{\delta Z_G}{\delta \phi_B})^2 \times [\sigma(\phi_B)]^2 \quad (6)$$

According to Eq. (4-6), we can get the standard errors of the space coordinates. A computer program was designed to apply the above formulas to obtain the accuracy of the space coordinates. Additionally, the mean square error (m.s.e) in different planes can be calculated by the forms;

$$\sigma_R = [(\sigma_X)^2 + (\sigma_Y)^2 + (\sigma_Z)^2]^{0.5} \quad (7)$$

The final results for space coordinates (X_G, Y_G, Z_G) and the final mean square errors (m.s.e) {$\sigma(X_G)$, $\sigma(Y_G)$, $\sigma(Z_G)$, σ_R} for twenty targets of group (I) and for thirty-five targets of group (II) were shown in Table 1 and 2, respectively.

Photogrammetric procedures with two non-metric photographs: We use Yashka (EZS-70) non metric camera and Kodak film speed is 100 ASA. (American Standard Association), film speed describes film's threshold sensitivity to light to take many photographs of the historical wall of Moid Shikh Mosque. The focal length (f) is 50 mm and the image format of the roll film is 24×36 mm. The only available way for getting digital image is the use of a Personal Computer (PC) and a good scanner using resolution 1000 dpi while the storage used area in hard disk for one photograph about 70 MB. The basic function of a scanner is to convert a hardcopy photograph to digital format (that is, softcopy format).

Scanners are used to reflect the image paper print or the film to models in the computer. The photographs were converted to digital format by using Genius advanced

Table 1: The ground coordinates (m) for group (I) of targets points and their m.s.e (mm) of the historical wall

No. of control points	Ground coordinates from intersection method (m)			σ (mm)			
	X_G	Y_G	Z_G	X	Y	Z	Vector (R)
47	1000.340	25.837	516.253	0.4	1.7	1.8	2.5
2	1000.446	17.878	516.352	0.4	0.8	1.8	2.0
1	1000.491	15.470	516.360	0.4	0.6	1.8	1.9
48	1002.139	25.843	516.233	0.4	1.7	1.7	2.5
4	1004.212	17.899	516.275	0.6	0.8	1.7	2.0
3	1004.229	15.500	516.282	0.6	0.6	1.7	1.9
49	1003.974	25.824	516.199	0.5	1.7	1.7	2.4
50	1006.390	25.812	516.164	0.7	1.6	1.7	2.4
51	1008.207	25.808	516.155	0.9	1.6	1.7	2.5
6	1008.505	17.886	516.207	0.9	0.8	1.7	2.1
5	1008.540	15.457	516.222	0.9	0.6	1.7	2.0
8	1012.823	17.883	516.152	1.3	0.8	1.7	2.3
7	1012.838	15.479	516.161	1.3	0.7	1.7	2.2
54	1013.082	25.500	516.101	1.3	1.6	1.7	2.6
55	1014.884	25.716	516.076	1.5	1.6	1.7	2.7
56	1016.702	25.712	516.054	1.6	1.6	1.7	2.9
10	1017.162	17.567	516.080	1.7	0.9	1.7	2.5
9	1017.195	15.438	516.083	1.7	0.7	1.7	2.5
57	1018.518	25.660	516.032	1.8	1.6	1.7	3.0
58	1020.326	25.463	516.010	2.0	1.6	1.7	3.1

Table 2: The ground coordinates (m) for group (II) of targets points and their m.s.e (mm) of the historical wall

No. of control points	Ground coordinates from intersection method (m)			σ (mm)			
	X_G	Y_G	Z_G	X	Y	Z	Vector (R)
12	1023.511	17.573	515.977	0.6	1.1	2.7	3.0
11	1023.661	15.431	515.978	0.6	0.8	2.7	2.9
20	1024.424	22.052	515.978	0.7	1.9	2.7	3.4
19	1024.741	23.863	515.991	0.7	2.2	2.7	3.6
21	1026.638	24.185	515.966	1.0	2.3	2.7	3.7
25	1027.766	20.064	515.920	1.2	1.6	2.7	3.3
13	1027.777	15.425	515.917	1.2	0.8	2.7	3.1
23	1027.780	21.753	516.283	1.2	1.8	2.8	3.5
14	1027.782	17.878	515.920	1.2	1.2	2.7	3.2
27	1029.993	19.931	515.880	1.5	1.5	2.7	3.5
26	1030.006	20.983	515.891	1.6	1.7	2.7	3.6
45	1032.179	17.875	515.848	1.9	1.2	2.7	3.5
29	1032.221	15.417	515.851	1.9	0.8	2.7	3.4
30	1032.281	20.081	515.851	1.9	1.6	2.7	3.7
34	1032.861	19.139	515.839	2.0	1.4	2.7	3.7
31	1033.239	20.192	515.838	2.1	1.6	2.8	3.8
65	1034.259	25.429	515.785	2.3	2.5	2.8	4.4
33	1034.320	19.899	515.817	2.3	1.6	2.8	3.9
32	1035.796	19.045	515.793	2.5	1.4	2.8	4.0
35	1036.273	20.004	515.790	2.6	1.6	2.8	4.2
46	1036.458	15.407	515.774	2.7	0.9	2.8	4.0
44	1036.468	17.859	515.779	2.7	1.2	2.8	4.1
66	1036.653	25.418	515.736	2.7	2.5	2.8	4.6
36	1037.310	19.306	515.772	2.8	1.5	2.8	4.3
37	1038.408	19.928	515.755	3.0	1.6	2.9	4.5
67	1039.065	25.458	515.681	3.1	2.6	2.9	5.0
39	1039.488	19.311	515.736	3.2	1.5	2.9	4.6
70	1040.296	25.487	515.654	3.4	2.6	3.0	5.2
43	1040.313	15.389	515.718	3.4	0.9	3.0	4.6
42	1040.368	17.855	515.722	3.4	1.3	3.0	4.7
38	1040.379	19.409	515.724	3.4	1.6	3.0	4.8
40	1041.300	19.359	515.711	3.6	1.6	3.0	5.0
68	1042.128	25.511	515.620	3.8	2.7	3.1	5.6
41	1042.383	19.908	515.691	3.9	1.7	3.1	5.2
69	1043.920	25.502	515.589	4.2	2.8	3.2	6.0

scanner color page-HR6X. This scanner has true optical resolution up to 600 dpi with interpolation up to 19200 dpi. It includes a transparency adapter (TPA) with auto-density technology; this technology can automatically adjust and enhance the scan color of slides and films to create high quality.

Scanner specifications

- Scanner type Genius HR6X color page
- True optical resolution: 600×1200 dpi
- Transparency adapter (TPA) included for multiple positive and negative scanning
- Scanning bit depth: 48-bit input hardware color depth output
- Supported with USB interface
- Supported Windows XP/Me/2000/98

Personal computer specifications

- Processor intel PIII 2.8 GH
- RAM: 256 MB
- Monitor 17 inch
- Display adapter: svga 32 MB
- Hard disk 80 GB
- Operation system Windows 98

This personal computer is compatible with IBM computer and with the scanner software. The measurements of the image coordinates for the points obtained from Auto-CAD version (14) computer program and recording in EXCEL program RMS manual for three models and their image coordinates will be shown later.

In this stage, a computer program using the bundle adjustment with self-calibration technique was applied to calculate the space coordinates (X_{ph}, Y_{ph}, Z_{ph}) and the root mean square errors for the target points. Three computer programs were used to fulfill the above requirements. These programs are Bundle adjustment with self-calibration (BSC) program, Auto-CAD-14 and Computer programs written with SQL language (Excel).

The BSC program developed by Novak 1991, which was designed by (c) under Unix programming language. This program solved the photogrammetric triangulation problem by bundle adjustment with self-calibration technique. Figure 6 shows the structure of BSC program.

The BSC program was used by providing it with a file containing the photo coordinates of all points in the stereopair (*.icf), a file containing the space coordinates of all control point (*.gcf), a file containing the camera parameters (*.cam) and a file containing the approximations for the orientation parameters (*.apx). The

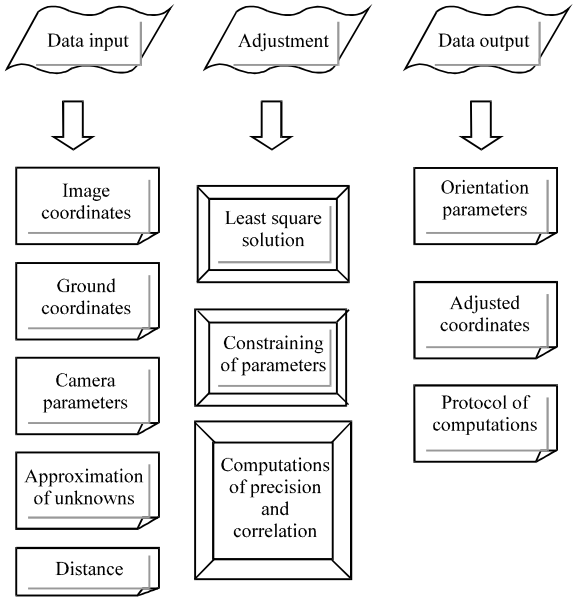

Fig. 6: Structure of BSC program

output of the program is a DXF file containing the space coordinates of all the points (control and check). We can get the coordinates for checkpoints by using AutoCAD program and write these coordinates in RMS Excel program to find the difference in X, Y and Z directions.

Thirty photographs were taken with different locations taking into consideration the object distance (D). From each location, we take five photographs for the same part of the historical wall of Moid Shikh mosque and the best clear one had chosen to be used in this study.

Three models have been chosen from the available photographs with different overlap ratio. The object distance (D) was chosen to be 16 m because it is the only available distance in the site of the field work:

First model: This model contain two photographs No. (001, 012), each one have 21 targets and the base distance (B) between the two stations was 15 m, then the overlap ratio was 65%.

Second model: This model contain two photographs No. (015, 025), which have 17 and 13 targets respectively and the base distance (B) between the two stations was 24 m, then the overlap ratio was 83%.

Third model: This model contain two photographs No. (002, 034), each one has 21 targets and the base distance (B) between the two stations was 7 m, then the overlap ratio was 59%.

The print format obtained the print of the non-metric camera is 15×10 cm. This print photographs were scanned

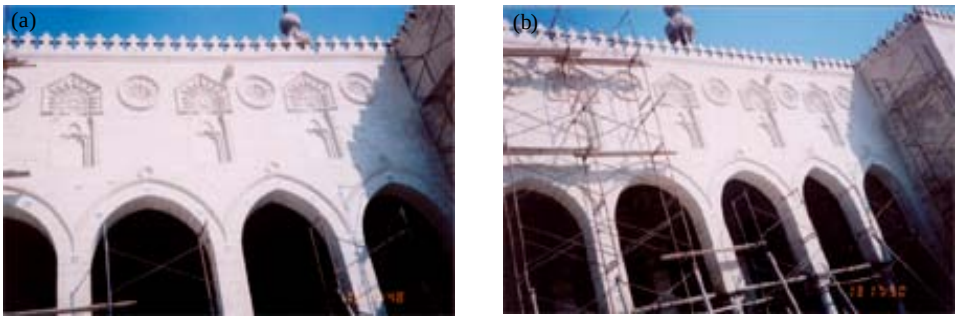

Fig. 7: (a) The left non-metric photograph No. 001 and (b) The right non-metric photograph No. 012

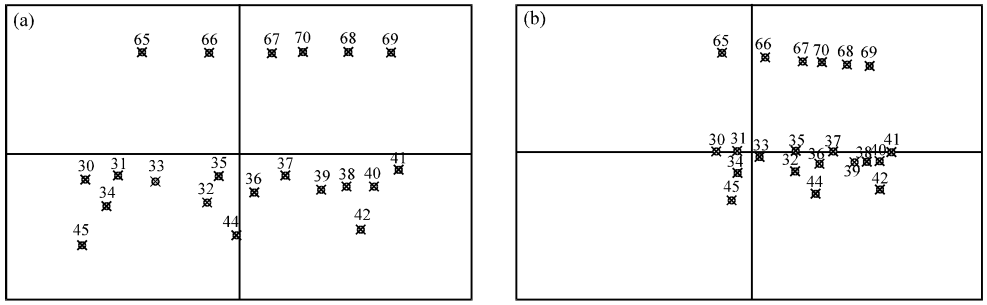

Fig. 8: (a) The positions of the targets for No. 001 and (b) the positions of the targets for No. 012

using Genius HR6X color page scanner with high resolution 1000 dot per inch (dpi) to change the photographs from print to digital format (pixel format). These digital photographs were transferred to the AutoCAD program. The final digital format obtained in AutoCAD program were equal the same size of the negative film format 24×36 mm to be compatible with the used camera focal length (f = 50 mm). The photo coordinates which are used, as input data of the BSC computer program should be measured from the principal point of the metric camera, but in our study because, we use a non-metric camera we measured the photo coordinates from the point of symmetry (center of each photograph) by using AutoCAD program. For example, Fig. 7a and b show the non-metric photographs and Fig. 8a and b show the positions of the targets using in model one.

ANALYSIS OF EXPERIMENTAL WORK

The number of control points: The main objective of this test is to investigate the effect of increasing the number of control points on the RMS in X, Y and Z directions as well as space length (L), this study will be done for the three models.

$$V_{x_i} = V_{G_i} - V_{ph_i} \quad ; \quad (R.M.S)_X = \sqrt{\frac{\sum_{i=1}^{n} V^2}{n}}$$

Where:

$(RMS)_X$: The root mean square errors of the targets in the X direction

n : No. of targets

Similar formulas were used for Y-direction, the Z-direction and the space length (L) to compute the root mean square error values for each direction. Many relations have been done in this study, we choose for each model two deferent positions, position (1) and position (2) for the control points. The final results of the accuracy obtained from the study were shown in Table 3-5 for models 1, 2 and 3, respectively. Figure 9-11a, b show the relationship between the number of control points and RMS for models 1, 2 and 3 at two positions (1) and (2) for every model, respectively.

According to the Fig. 9-11, we can see that in each model:

- The relations are approximately constant for all the models and all the positions.

Table 3: The RMS in cm for (X, Y, Z) directions and space vector (R) for model one (overlap 65%)

No. of control points	Control points	$(RMS)_X$	$(RMS)_Y$	$(RMS)_Z$	$(RMS)_R$
Position (1)					
3 control points	(42-45-65)	16.0	12.0	6.2	20.9
4 control points	(42-45-65-68)	5.4	4.1	5.1	8.4
5 control points	(32-42-45-65-68)	5.3	4.2	4.3	8.0
6 control points	(30-41-42-45-65-69)	4.0	4.6	4.0	9.4
Position (2)					
3 control points	(33-38-44)	11.9	15.3	11.8	22.6
4 control points	(33-38-44-67)	6.9	6.6	7.0	11.9
5 control points	(32-33-38-44-67)	7.2	6.9	7.5	12.4
6 control points	(32-33-38-44-67-69)	5.4	4.6	6.5	9.6

Table 4: The RMS in cm for (X, Y, Z) directions and space vector (R) for model two (overlap 83%)

No. of control points	Control points	$(RMS)_X$	$(RMS)_Y$	$(RMS)_Z$	$(RMS)_R$
Position (1)					
3 control points	(4-47-56)	5.2	11.4	10.3	16.2
4 control points	(4-6-47-56)	5.1	10.8	8.9	14.4
5 control points	(4-6-47-50-56)	4.5	8.4	6.2	11.4
Position (2)					
3 control points	(8-47-56)	6.1	8.8	6.3	14.1
4 control points	(4-8-47-56)	6.0	9.1	6.8	12.8
5 control points	(6-8-47-51-56)	5.1	7.7	6.2	11.1

Table 5: The RMS in cm for (X, Y, Z) directions and space vector (R) for model three (overlap 59%)

No. of control points	Control points	$(RMS)_X$	$(RMS)_Y$	$(RMS)_Z$	$(RMS)_R$
Position (1)					
3 control points	(23-33-45)	4.70	9.25	10.19	14.5
4 control points	(21-23-33-45)	2.61	6.33	8.22	10.7
5 control points	(21-23-25-33-45)	1.68	4.82	5.62	7.6
Position (2)					
3 control points	(14-23-33)	3.73	9.50	8.52	13.3
4 control points	(14-23-33-45)	3.62	8.26	6.23	11.0
5 control points	(14-23-25-33-45)	3.74	7.53	5.81	10.2

- The relations are semi parallel for each position; that's mean the relations are nearly the same for all figures.
- These relations approved that, when the number of control points increasing, the RMS is decreasing and consequently the accuracy is increasing.

The ratio of the base distance (B) to the object distance (D): We can conclude from Table 6, when B =15 m and D = 16 m, (B/D ≅ 1.0) in model one (overlap 65%), we get the best accuracy for the computed ground coordinates. When B = 24 m and D = 16 m (B/D ≅ 1.5) in model two (overlap 83%), we get the worst accuracy in the computed ground coordinates. While the accuracy comes in between for the computed ground coordinates when B = 7 m and D = 16 m (B/D ≅ 0.5) in model three (overlap 59%).

According to Fig. 12, which shows the relations between B/D ratio against RMS in X, Y, Z and R directions, we can see that:

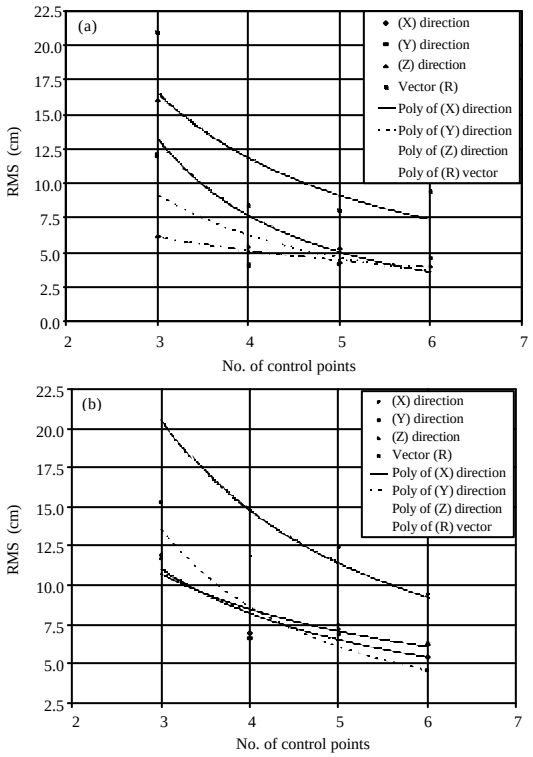

Fig. 9: The relationship between the number of control points and RMS in check points for model one (a) position (1) and (b) position (2)

- The relations between the values of B/D ratio and RMS are nearly the same for Y, Z and R direction.
- The relations are directly proportionally in the range of 0.5≤ (B/D) ratio ≤ 1.0 (i.e., when the values B/D ratio is increasing, the accuracy is increasing), while the relations are inversely proportionally in the range of 1.0≤ (B/D) ratio ≤ 1.5 (i.e., when the value of B/D ratio is increasing, the accuracy is decreasing).
- The relation in X-direction approved that, when the values of B/D in the range 0.5≤ (B/D) ratio ≤ 1.0 the relation between B/D ratio and RMS is inversely proportionally (i.e., when the value of B/D ratio is increasing, the accuracy is decreasing). While the relation is directly proportionally when the values of B/D in the range 1.0≤ (B/D) ratio ≤ 1.5 (i.e., when the values of B/D ratio is increasing, the accuracy is increasing).
- From the above observations we see that, the relation in X-direction is the only one which is not matched with the other relations and that may be due to the big effect of the angle of convergence (ϕ) on the accuracy in X-direction.

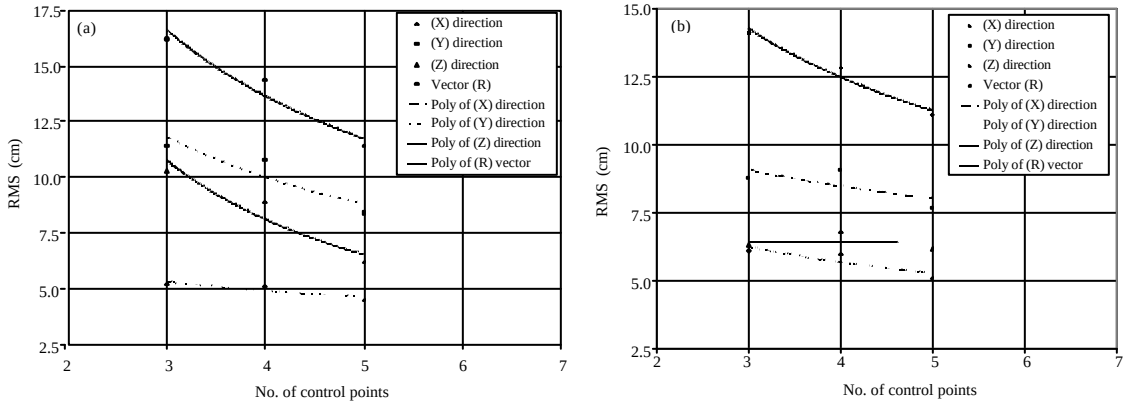

Fig. 10: The relationship between the number of control points and RMS in check points for model two (a) (position (1) and (b) position (2)

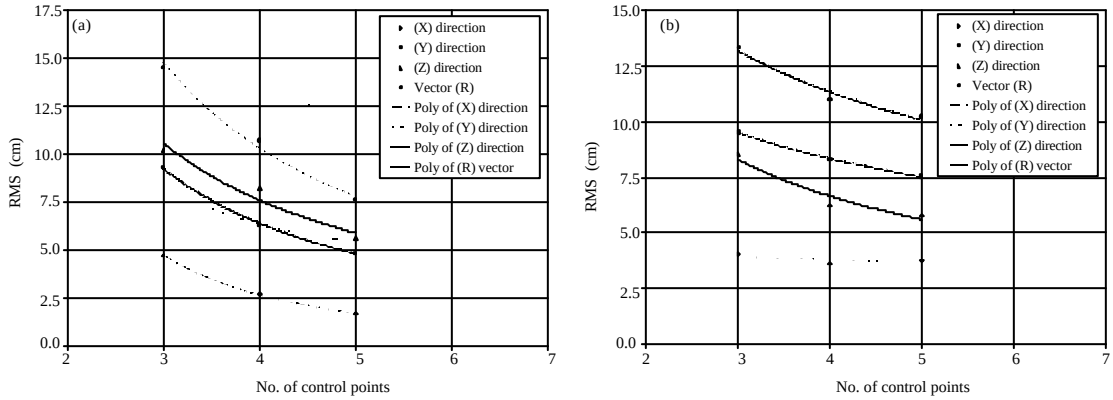

Fig. 11: The relationship between the number of control points and RMS in check points for model three (a) position (1) and (b) position (2)

Table 6: The most probable values of the exterior orientation parameters and calculate average of RMS in X, Y, Z as well as R-directions of non-metric camera and (B/D) ratio

		Model (1) (overlap 65%)		Model (2) (overlap 83%)		Model (3) (overlap 59%)	
		Left	Right	Left	Right	Left	Right
The length of the base line (m)	B	15		24		7	
The object distance (m)	D	16		16		16	
(B/D) ratio		1.0		1.5		0.5	
The coordinates of the	X_L	1032.092	1017.118	1022.785	998.644	1032.901	1026.182
exposure stations (m)	Y_L	9.467	9.695	9.578	9.663	10.060	9.934
	Z_L	499.625	497.380	497.881	497.155	499.325	502.790
The orientation elements (rad)	ω	35.89	30.56	28.46	32.98	33.84	38.66
	ϕ	-14.53	-37.07	25.00	-17.24	-3.72	-9.34
	κ	-1.11	-0.13	4.76	-0.29	-1.53	0.17
The root mean	$(RMS)_X$	6.12		5.48		3.71	
square errors (cm)	$(RMS)_Y$	5.73		9.06		7.77	
	$(RMS)_Z$	6.36		7.01		7.27	
	$(RMS)_R$	10.67		12.75		11.36	

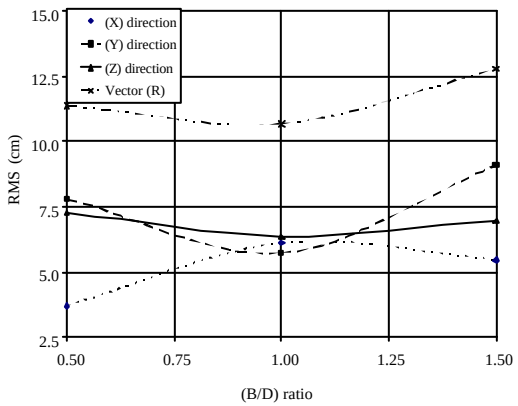

Fig. 12: The relationship between B/D ratio against the RMS in X, Y, Z and R directions

CONCLUSIONS AND FUTURE WORK

This study evaluates both of the effect of the number of control points as well as the effect of the ratio of the base line distance (B) over the object distance (D) [(B/D) ratio] on the accuracy obtained from the ground coordinates using non-metric photographs for documenting historical buildings. We choose a wall of Moid Shikh historical mosque located in Ghoria, beside Bab Ziwala, Cairo, Egypt as a test object. From the previous analysis we can conclude that for evaluated the effect of the number of control points on the accuracy obtained from non-metric photographs for documenting historical buildings, when the number of control points increasing, the accuracy is increasing. The effect of the ratio of the base line distance (B) over the object distance (D) [(B/D) ratio] on the accuracy obtained using Non-Metric photographs for documenting historical buildings, the relations Y, Z and R direction are directly proportionally in the range of $0.5 \leq$ (B/D) ratio ≤ 1.0, while the relations are inversely proportionally in the range of $1.0 \leq$ (B/D) ratio ≤ 1.5. Only the relation in X-direction is not matched with the other relations, that is may be due to the big effect of the angle of convergence (ϕ) on the accuracy in X-direction.

Future works will be focused on the effect of the angle of convergence (ϕ) on the accuracy, as well as the effect of more number of control points on the accuracy.

REFERENCES

Atkinson, K.B., 2001. Theory of Close Range Photogrammetry in a Book Close Range Photogrammetry and Machine Vision. Chapter 2, Whittles Publishing, Scotland, UK., pp: 384.

Jechev, D., 2004. Close-range Photogrammetry with Amateur Camera. 20th ISPRS Congress. Vol. XXXV. Part B8. July 12-23, Istanbul, Turkey, Youth Forum Papers, pp: 136-136.

Karara, H.M. and Y.I. Abdel-Aziz, 1974. Accuracy aspects of non-metric imageries. Photogrammet. Eng., 40: 1107-1117.

Mofitt, F.H. and E.M. Mikhail, 1980. Photogrammetry. 3rd Edn., Harper and Row, Inc., New York, USA., ISBN: 0-700-22517-X.

Nutto, M. and K. Ringle, 2001. Photogrammetric documentation of the castle of heidelberg from data capture to information system. Proceedings of the XVIII International Symposium of CIPA 2001 Potsdam (Germany), Surveying and Documentation of Historic Buildings-Monuments-Sites. September 18-21, Traditional and Modern Methods, pp: 624-629.

Wolf, P.R. and B.A. Dewitt, 2000. Elements of Photogrammetry, with Applications in GIS. 3rd Edn., McGraw-Hill, Boston, ISBN: 0072924543.